NASA TECHNICAL NOTE

NASA TN D-3224

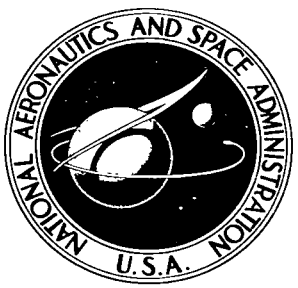

NASA TN D-3224

MAGNETIC BREAKDOWN IN A FINITE ONE-DIMENSIONAL MODEL

INFINITE POTENTIAL RELAXED

by Gabriel Allen

Lewis Research Center
Cleveland, Ohio

NATIONAL AERONAUTICS AND SPACE ADMINISTRATION • WASHINGTON, D. C. • MARCH 1966

NASA TN D-3224

MAGNETIC BREAKDOWN IN A FINITE ONE-DIMENSIONAL MODEL - INFINITE POTENTIAL RELAXED

By Gabriel Allen

Lewis Research Center
Cleveland, Ohio

NATIONAL AERONAUTICS AND SPACE ADMINISTRATION

For sale by the Clearinghouse for Federal Scientific and Technical Information
Springfield, Virginia 22151 – Price $0.40

MAGNETIC BREAKDOWN IN A FINITE ONE-DIMENSIONAL MODEL - INFINITE POTENTIAL RELAXED

by Gabriel Allen

Lewis Research Center

SUMMARY

Exact solutions have been obtained for a model representing an electron in a one-dimensional periodic potential acted on by a transverse uniform magnetic field. The periodic potential is approximated by a finite chain (20 atoms long) of "periodic" square wells. Within this chain, the parabolic potential due to the magnetic field was approximated by a parabolic square-well potential. The infinite potential at each end of the chain, which was used in a previous report to cut off the chain sharply, is relaxed and the true magnetic parabolic potential was used outside of the chain. Eigenvalues and wave functions are computed for the case of equal widths of wells and hills in the periodic part of the potential. A reasonably consistent interpretation of the behavior of the wave functions is presented with crossing-like behavior between zero field energy bands being a likely part of the interpretation.

INTRODUCTION

In a previous report (ref. 1) exact quantum-mechanical solutions were obtained for a model representing an electron in a one-dimensional periodic potential acted on by a uniform transverse magnetic field. The results of an analysis of the eigenvalues and wave functions of this system showed that the model seemed to be capable of following certain magnetic breakdown effects in some detail. It was possible to see the increasing influence of the magnetic fields on the behavior of the states by following individual states from zero magnetic field (where the periodic band structure properties control the behavior of the system) to magnetic fields larger than Blount breakdown fields.

For the system in reference 1, the Schroedinger equation was reduced to a one-dimensional problem with an effective potential of the form shown in figure 1 (called a parabolic square-well potential). In the figure, the depth of the periodic potential well is denoted by V_0 and the magnetic step in the potential is denoted by V_0' where

$$V_0' = \frac{1}{2m}\left(\frac{eH_z}{c}\right)^2 a^2 \tag{1}$$

where a is the period.

The absence of periodicity meant that the number of matching conditions (and thereby the rank of the determinant used for the determinantal compatibility condition) increased with the length of the chain. The absolute cutoff condition, which may be written as

$$V\left[(N + 1)a - w\right] = \infty \tag{2}$$

was imposed to keep the number of computations down to a manageable level. In equation (2), N is the number of atoms in one-half of the chain, and 2w is the width of the periodic potential well.

The main effect of this condition appeared to be that wave functions belonging to eigenvalues near $V_0 + N^2V_0'$ were forced to zero near the cutoff region at the end of the chain. The relaxing of the absolute cutoff condition should therefore improve the model. To this end, a program for determining eigenvalues and wave functions for an effective potential of the form shown in figure 2 was undertaken. The program was completed and the results have been used to try to interpret those effects in both the eigenvalues and wave functions arising from the cutoff condition.

Significant changes in the results were not expected, and the main features of the preceding model were found again. However, the effects of the possible interchange of properties between different bands were not considered in reference 1, and the likelihood of such events permitted a more detailed interpretation of the results to be made than in the preceding report.

SYMBOLS

A_M constant multiplying wave function in pure magnetic region

a period

c velocity of light

D_N functional form of determinantal compatibility condition

$D_\nu(\xi)$ ν^{th} order parabolic cylinder function

E parametrized quantity used like energy, see eq. (6)

e charge of electron

G $\sqrt{|g|}$

g defined by eqs. (11) and (12)

H magnetic field strength

$\vec{H}$	magnetic field
H_B	Blount breakdown value of magnetic field
H_z	magnitude of z-component of magnetic field
$\hbar$	Dirac h, Planck's constant/2π
k_z	component of wave vector
m	mass of electron
N	number of atoms in one-half of chain
n	integer defining level of state in band
r	cyclotron radius
$S_0^w, \bar{S}_0^w$	defined by eqs. (A11) and (A12)
$S_n^h, \bar{S}_n^h$	defined by eq. (A13)
$S_n^w, \bar{S}_n^w$	defined by eq. (A14)
V_0	well depth of periodic potential
V_0'	magnetic step in potential
$V(x')$	total potential
w	half-width of periodic potential well
x,y,z	coordinates
ϵ	actual eigenvalue of system
$\lambda(x')$	wave function
ν	defined by eq. (15)
ξ	defined by eq. (16)
ω_c	cyclotron frequency

Subscripts:

M pure magnetic

N last period in periodic potential region

n n^{th} period

Superscripts:

h hill

w well

R reduced

$\overline{0}$ sign of appropriate g
$+$

MODEL DESCRIPTION

Most of the characteristics of the model are the same as in reference 1. In particular, in the region

$$-\left[(N+1)a - w\right] \leq x' \leq \left[(N+1)a - w\right]$$

the same parabolic square-well potential applies as in reference 1. (Compare this region in figs. 1 and 2.) However, in reference 1, at

$$x' = (N+1)a - w$$

the cutoff condition given by equation (2) is applied. This condition may be described as an absolute cutoff in the sense that it has the effect of keeping the electron entirely inside the "box" so that for

$$|x'| > (N+1)a - w$$

the wave function $\lambda(x')$ is zero.

In this report, the absolute cutoff condition is partially relaxed (by keeping the "pure" magnetic potential) to allow the system to penetrate into the region $|x'| > (N+1)a - w$. However, the periodic part of the potential is still cut off in order to keep the number of matching conditions finite. In this region, the effective potential will subsequently be called pure magnetic.

Relaxing the absolute cutoff condition makes for an improved model in the obvious sense of releasing the electron from its "box." However, the boxing-in aspect had the advantage of providing a natural starting point for the individ-

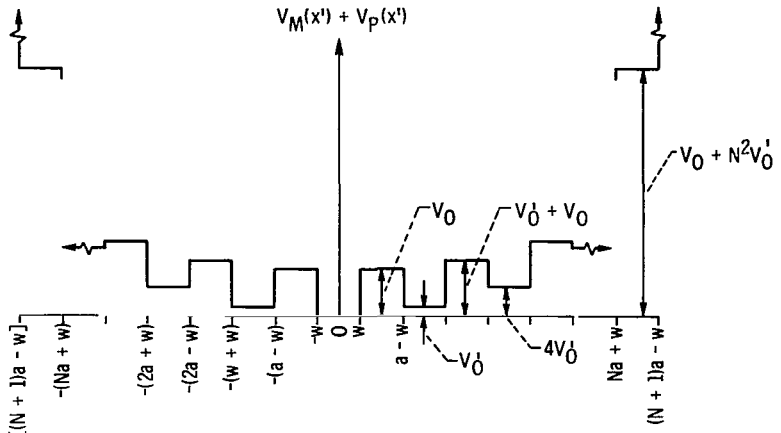

Figure 1. - Form of potential given by parabolic square well with absolute cutoff.

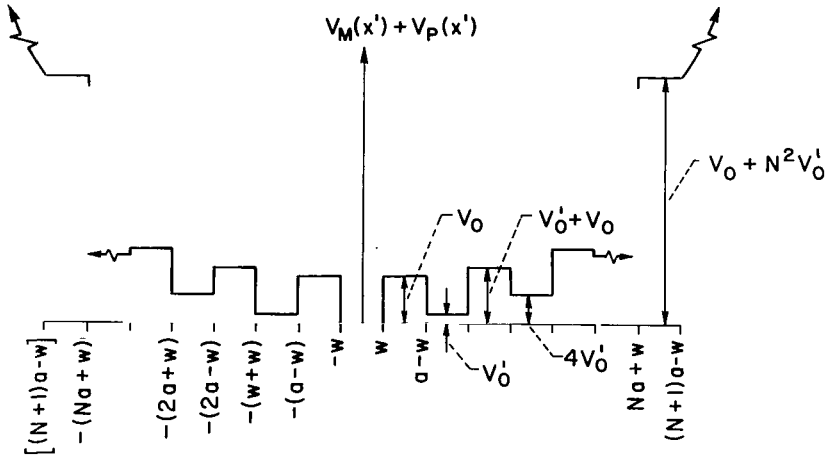

Figure 2. - Form of potential due to parabolic square well without absolute cutoff, w = a/4.

ual states at $\vec{H} = 0$. The identity of these zero-field states was preserved and the individual states could be followed as $\vec{H}$ increased to Blount breakdown values.

In the present model, the absolute cutoff condition is replaced by the pure magnetic potential

$$V(x') = \frac{2m}{\hbar^2}\left(\frac{1}{2}m\omega_c^2 x'^2\right) \tag{3}$$

in the region $|x'| \geq (N + 1)a - w$, where the cyclotron frequency is

$$\omega_c = \frac{eH_z}{mc} \tag{4}$$

When figure 2 is referred to, it can be seen that if $\vec{H} = 0$ there will be

no bound states at all; however, any finite $\vec{H}$, no matter how small, will bind the system. Thus, there can be no easy transition from small fields to zero field.

There is no good reason to give up this advantage of the cutoff model. For the lower lying states, the absolute cutoff condition has very little effect on the system since for the fields studied in reference 1 the finite potential barrier was already very large at $x' \lesssim (N + 1)a - w$. Thus, the main advantage gained by relaxing the absolute cutoff was in examining the behavior of higher states (at comparatively small magnetic fields) whose amplitudes would still be appreciable in this vicinity if not forced to zero by the cutoff. (At high magnetic fields, the cyclotron radius becomes so small that the wave function has a very small amplitude near the periodic cutoff except for states at rather high levels.) Now it is desirable to follow the behavior of states which flank the first energy gap (band gap) at zero field up through higher fields. At relatively low fields, those states would come under the heading of low-lying states as described previously. There is thus no reason to relax the absolute cutoff condition at small fields and the eigenvalues for zero field computed using this condition will be retained in this model.

A proper way to effect a smooth transition would be to start with a fully periodic potential (a "chain" of infinite length) at zero field and then introduce a periodic cutoff potential of monotonically decreasing length as H increases. Computational difficulties make such a procedure impractical.

To summarize then, the model used herein is the parabolic square well with periodic cutoff of figure 2 for $\vec{H} > 0$ and the periodic potential in a box of figure 1 at $\vec{H} = 0$.

SOLUTION OF WAVE EQUATIONS

After the standard reduction to one dimension, the wave equation for the physical system becomes

$$\frac{d^2\lambda}{dx'^2} + \left[E - V(x')\right]\lambda = 0 \tag{5}$$

where $V(x')$ is the potential shown in figure 2 and

$$E = \frac{2m}{\hbar^2}\left(\epsilon - \frac{\hbar^2 k_z^2}{2m}\right) \tag{6}$$

where ϵ is the actual eigenvalue of the system and k_z is that component of the wave vector $\vec{k}$ which is parallel to the magnetic field $\vec{H}$. These equations and definitions are identical with equations (23) and (21) respectively in reference 1, except for the fact that in this report the cutoff condition (2) is replaced by the condition

$$V(x') = \frac{2m}{\hbar^2}\left(\frac{1}{2} m \omega_c^2 x'^2\right) \qquad |x'| > (N + 1)a - w \tag{7}$$

The solution to equation (5) in the regions of constant potential contained in the interval $0 \leq x' \leq Na + w$ are of the same form as in reference 1 and are summarized below for the even solutions:

$$\lambda_0^w(x') = B_0^w \cos G_0^w x' \tag{8}$$

where $-w \leq x' \leq w$,

$$\lambda_n^w(x') = \begin{cases} \dfrac{A_n^w}{G_n^w} \sinh G_n^w \left[x' - (na - w)\right] + B_n^w \cosh G_n^w \left[x' - (na - w)\right] & g_n^w < 0 \\ A_n^w \left[x' - (na - w)\right] + B_n^w & g_n^w = 0 \\ \dfrac{A_n^w}{G_n^w} \sin G_n^w \left[x' - (na - w)\right] + B_n^w \cos G_n^w \left[x' - (na - w)\right] & g_n^w > 0 \end{cases} \tag{9}$$

where $na - w \leq x' \leq na + w$, and

$$\lambda_n^h(x') = \begin{cases} \dfrac{A_n^h}{G_n^h} \sinh G_n^h \left[x' - (na + w)\right] + B_n^h \left[x' - (na + w)\right] & g_n^h < 0 \\ A_n^h \left[x' - (na + w)\right] + B_n^h & g_n^h = 0 \\ \dfrac{A_n^h}{G_n^h} \sin G_n^h \left[x' - (na + w)\right] + B_n^h \cos G_n^h \left[x' - (na + w)\right] & g_n^h > 0 \end{cases} \tag{10}$$

where $na + w \leq x' \leq (n + 1)a - w$. In equations (8) to (10),

$$g_n^w = \frac{2m}{\hbar^2}\left(\epsilon - \frac{\hbar^2 k_z^2}{2m} - n^2 V_0'\right) \tag{11}$$

$$g_n^h = \frac{2m}{\hbar^2}\left(\epsilon - \frac{\hbar^2 k_z^2}{2m} - n^2 V_0' - V_0\right) = g_n^w - \frac{2m}{\hbar^2} V_0 \tag{12}$$

$$G = \sqrt{|g|} \tag{13}$$

Note that in this report equation (10) also applies in the region of the last hill, $Na + w \leq x' \leq (N + 1)a - w$, unlike the case in reference 1 which requires a special form for this region.

For $x' \geq (N + 1)a - w$, the harmonic oscillator potential $\frac{1}{2} m\omega_c^2 x'^2$ governs the behavior of the system and the solution becomes

$$\lambda_M(x') = A_M D_\nu(\xi) \tag{14}$$

where $D_\nu(\xi)$ is the ν^{th} order parabolic cylinder function (ref. 2), A_M is a constant, and

$$\nu = \frac{\epsilon}{\hbar\omega_c} - \frac{1}{2} \tag{15}$$

$$\xi = \left(\frac{2m\omega_c}{\hbar}\right)^{1/2} x' \tag{16}$$

The subscript M denotes the fact that in this region the potential is pure magnetic.

The modifications that this requires in the matching conditions and their use in computing eigenvalues are shown in appendix A. The use of Weber functions of high order introduced some special difficulties in the computations, which are discussed in appendix B. As in reference 1, the eigenvalues actually computed are $\epsilon - \hbar^2 k_z^2/2m$ rather than ϵ.

WAVE FUNCTIONS

Wave functions were obtained in the usual way by finding the coefficients in each region of constant potential in terms of an arbitrary coefficient which was the coefficient in the 0^{th} well, B_0^w. The procedure was essentially the same as described in reference 1 and need not be repeated here.

It should be noted that the wave functions were not normalized in the usual fashion. The difficulty lay in the fact that a proper normalization would require the evaluation of integrals of the form

$$\int_{\xi_M}^{\infty} D_\nu^2(\xi)\, d\xi$$

where

$$\xi_M = \left(\frac{2m\omega_c}{\hbar}\right)^{1/2} \left[(N+1)a - w\right]$$

There is no easy way to evaluate such integrals. Therefore, an incomplete normalization was used. The procedure consisted merely of neglecting the interval in the aforementioned integral and using the condition

$$\left(B_0^w\right)^2 \int_0^{(N+1)a-w} |\lambda(x')|^2 \, dx' = \frac{1}{2} \tag{16}$$

On the one hand, the use of this condition means that quantitative comparisons of the amplitudes of wave functions belonging to different eigenvalues are not valid. On the other hand, the kind of comparison that is suitable for the particular analysis desired can be made quite rigorously. For a given state, the amplitude is examined as a function of x' to determine in which part of the "crystal" the system has a comparatively larger probability of being found. Then, a similar examination is made for a different state in order to determine whether the two states have large and small amplitudes in the same regions. In this connection, it may be mentioned that for most states the neglected contribution to the normalization is quite small so that even the approximation to the absolute magnitudes of the amplitudes is good.

RESULTS AND DISCUSSION

Eigenvalues

The eigenvalues for various well depths are shown as a function of magnetic field strength $\vec{H}$ in figure 3. Since magnetic field strength is a common parameter, it was chosen as the ordinate in preference to V_0'. However, V_0' is also shown on the vertical scale to make it easier to compare these results with those in reference 1. The discontinuities in the slopes in the figures are due to the procedure used. For each V_0, computations were carried out for a few values of H and these eigenvalues were then connected by straight lines. It is convenient to let these lines represent the same "state" at different magnetic field strengths. As explained in the last section, the eigenvalues for $H_z = 0$ are those taken from the box model of reference 1. The Blount breakdown lines are shown on the figures as an aid in the analysis of the results. General quantum mechanical considerations ensure that alternate even and odd solutions occur (ref. 3). In a few cases, D_N oscillated near but not through zero for a series of trials for even solutions in an energy interval in which several odd solutions were found. In these instances, circles were placed between odd eigenvalues in the general vicinity of where the even eigenvalues must lie.

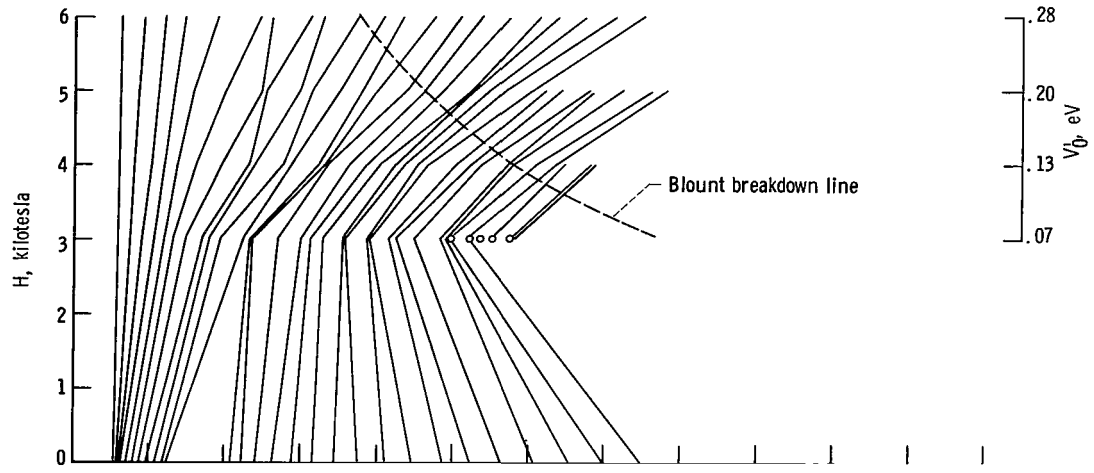

(a) Well depth of periodic potential, 5 electron volts.

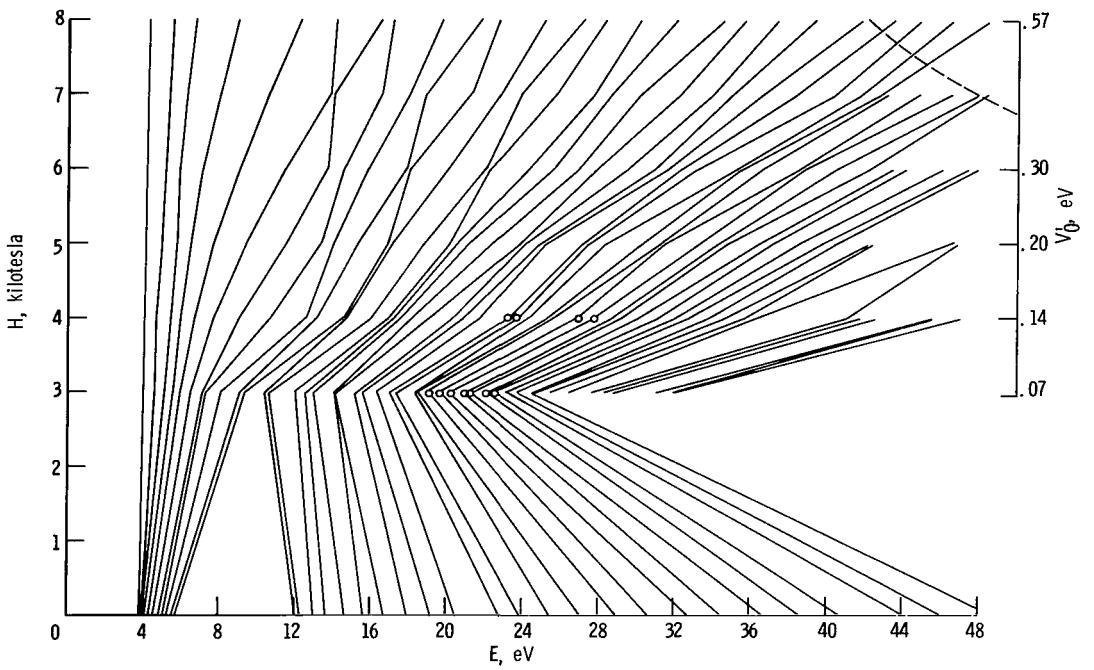

(b) Well depth of periodic potential, 10 electron volts.

Figure 3. - Eigenvalues as function of magnetic field strength.

From a comparison of figure 3 with the corresponding figure 3 of reference 1, it can be seen that at the same value of V_0' the density of eigenvalues in the second band increases when the absolute cutoff condition is relaxed. For very large fields, where the magnetic potential effectively boxes in the system anyway, the eigenvalues are essentially unchanged by the relaxing of the cutoff. The $H_z = 0$ values serve the purpose of identifying the band to which a particular eigenvalue belongs. However, there is clearly no longer a smooth transition from small field eigenvalues (for which the cutoff has been relaxed) to zero-field eigenvalues (for which the cutoff has been retained).

A fact should be noted here that was perhaps not made sufficiently clear in reference 1 to which it also applies. In computing the eigenvalues, an attempt would be made to find a value of ϵ which would make D_N (see appendix A) smaller than some preassigned value. This value of D_N which was chosen by trial and error was small enough to enable the boundary conditions to be satisfied by the wave functions. Although only those eigenvalues which satisfied this criterion were used in computing the wave functions, all of the values of ϵ at which D_N changed signs are presented in figure 3 both here and in reference 1. The identification of the band to which a given eigenstate belongs, together with its location in the band, is important even if the eigenvalue itself cannot be used in computing a satisfactory wave function.

Wave Functions

Before discussing the results of the calculations in this report, it might be of some interest to review briefly the results in reference 1. The general behavior of the wave functions was such that for $H \ll H_B$ (where H_B is the Blount breakdown value) the wave functions were greatly influenced by the periodic part of the potential. Thus the relative probability that the system would be found near compared to the probability that it would be found far from the cutoff was quite similar for states within the same band but changed drastically in going from a state on one side of the energy gap to a state just the other side of this gap. This change in behavior of the eigenstates on crossing an energy gap was always great even when the difference in the energies of the states flanking the gap at a fixed value of H was very small (see figs. 3(c) and 5 in ref. 1). As the magnetic field increased, however, the effect on the wave functions of crossing the energy gap became less pronounced until, at $H \approx H_B$, no discernible effect remained (see fig. 10, ref. 1).

It may be argued that the use of negative amplitudes was unnecessary. The reason for plotting the actual wave function rather than $|\lambda|$ or $|\lambda|^2$ was that it was easier to check visually the continuity of the slope across boundaries separating regions of different potential from $\lambda(x')$ than from either of the other choices.

When describing the strong effect of the periodic part of the potential on the behavior of these states, there is no intent to imply that any departure from the general behavior of electrons under the combined influence of periodic potentials and magnetic fields is being shown by this model. The magnetic field is the principal influence on the electron (ref. 4). All that the model is demonstrating is the difference between the effect of a magnetic field on free electrons and on electrons in a periodic potential. Electrons in states near the bottom of a band act very much like free electrons. Wave functions for such states are peaked near their cyclotron radius

$$r = \frac{\hbar k}{m\omega_c} \approx \frac{11.5\sqrt{n + \frac{1}{2}}}{\sqrt{H_z}}$$

where H_z is in kilotesla and n is the number identifying the level of the

state in the band (n = 1 for the ground state). For the model used here, these peaks are near the center of the effective potential.

As the states approach the top of the band, their behavior becomes less free and is more difficult to describe. However, at the bottom of the next band, a "free electron"-like behavior is to be expected again with peaks relatively near the center of the effective potential. For very large values of H, the effect of the periodic potential becomes less pronounced and the behavior of states near the top of a band will not be very different from those near the bottom of the successive band.

The preceding description omits any discussion of the possibility that the magnetic field can cause a crossing between states originally in different bands. Such an omission appears quite acceptable at first sight. If a given solution to a one-dimensional Schroedinger equation is a continuous function of a parameter, then the number of nodes of the solution will not be changed by a change in the parameter. Now the magnetic field H_z is a parameter of the wave function here, so a wave function that has, for example, 20 nodes when $H = 0$ will have 20 nodes when $H = 5$ kilotesla. Since the state represented by this function was in the first band at $H = 0$ (the state at the top of the first band has 21 nodes), the state which has 20 nodes when $H = 5$ kilotesla still has to be regarded as the same state (insofar as its location in the band is concerned).

This fact does not prevent the properties of the wave function at large H_z from being very much like those from another band at small H_z. A qualitative description of the situation can be made with the aid of figure 4(a), which is a schematic representation of the variation of the two distinct states 1 and 2 with an arbitrary parameter p. At a certain value p_c of the parameter, there is a near crossing of states 1 and 2. Under such circumstances, the wave functions for either of the two states may acquire a large admixture of properties of the other state. If such a mixing of properties occurs, then at some larger value of the parameter, for example p_o, the wave function for state 1 might have properties much like those which would be expected from an extrapolation of properties of state 2 when $p \ll p_c$ and vice versa. If states 1 and 2 are in different bands for $p \ll p_c$, the aforementioned pattern of events will be called an "interband transfer."

Figure 4(b) shows a possible two-stage interband transfer between a pair of states originally in the first band and a second pair originally in the second band.

The results of the present computations are shown in figures 5 and 6 for a V_o of 5 and 10 electron volts, respectively. In examining these figures, it should be kept in mind that the normalization was not complete so that quantitative comparisons between the amplitudes of different states at the same position may not be reliable. On the other hand, for a given state, the ratio of the amplitude near the periodic cutoff to the amplitude near the center will be independent of the absolute magnitude of the amplitude. A comparison of such ratios between two different states will, therefore, be reliable.

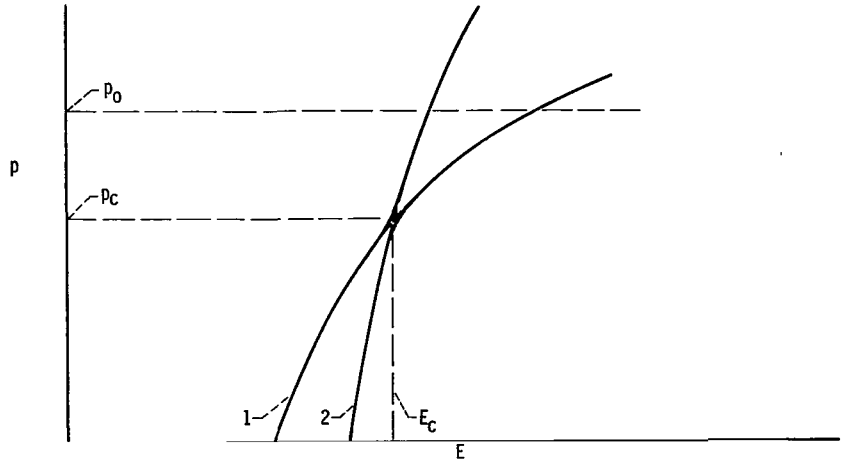

(a) Schematic possible transfer of properties between two states having a near-crossing.

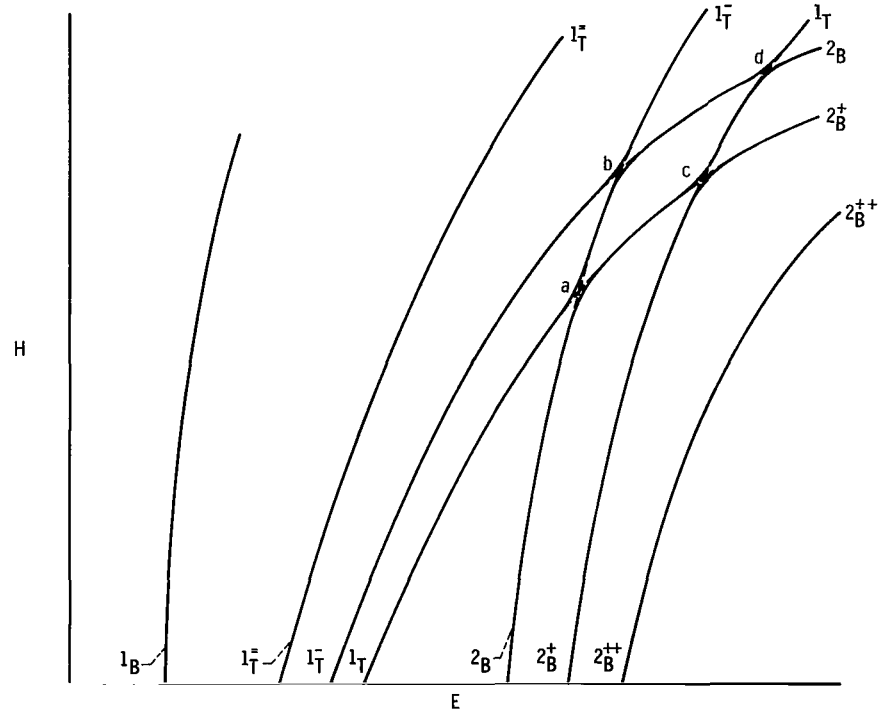

(b) Possible two-stage interband transfer between two states at top of first band and two states at bottom of second band. Transfer occurs between states 1_T and 2_B at (a), between 1_T and 1_T^- at (b), between 1_T and 2_B again at (d), and between 2_B and 2_B^+ at (c). For large values of magnetic field H, 1_T^- and 1_T states would have properties like states 2_B and 2_B^+, respectively, while 2_B and 2_B^+ would have properties like 1_T^- and 1_T, respectively. (State at bottom of first band, 1_B; state at top of first band, 1_T; state just below top of first band, 1_T^-; state just below state 1_T^-, $1_T^=$; state at bottom of second band, 2_B; state just above bottom of second band, 2_B^+; state just above state 2_B^+, 2_B^{++}.)

Figure 4. - Schematic representation of interband transfer.

In the remainder of the discussion the expression "_____ state in the _____ band" will mean "wave function corresponding to the _____ eigenvalue in the _____ band." Both the band and the position in the band refer to zero field.

Figure 5(a) may be selected for a detailed discussion. As can be seen from figure 3(a), a field strength of 3 kilotesla ($\ll H_B$) for $V_0 = 5$ electron volts. Thus, the influence of the periodic part of the potential should be discernible in figure 5(a). Examination of this figure shows that interband transfer is evident. The tenth odd state in the first band behaves like a state nearer the bottom of a band than the top. Such would be the case if the characteristics of states near the bottom of the second band crossed with the characteristics of some of the states near the top of the first band. The next two higher states (which, by the way, correspond to the top of the first band and bottom of the second band, respectively) act like states near the top of a band, which is in agreement with the description of transfer behavior. The next two states are both second band states. They do indeed behave like second band states and furthermore seem to behave like states not quite as near to the bottom of a band as the tenth odd state. The entire set of four states shown thus seems to be in complete conformity with the interpretation of interband transfer described in the preceding paragraphs.

Next figure 5(b) may be examined. The interpretation here is also in agreement with the overall picture described, but the results are less striking. The tenth odd state decidedly shows the behavior expected from a state near the top of a band so the crossing, in evidence for this state at 3 kilotesla, has disappeared at 4 kilotesla. The behavior of the other three states shown on the figure does not admit of a clear interpretation in terms of band position since no definite preference is shown for any particular part of the atomic chain. A comparison with figure 10(a) in reference 1 can be made to attempt to ascertain the effect of the absolute cutoff. That figure showed the behavior of wave functions in a potential having $V_0 = 5$ electron volts and $H = 3.8$ kilotesla, which is close to the conditions holding for figure 5(b) in this report.

It may be noted that the cutoff states seem to be showing transfer behavior since the states near the top of the first band at zero field exhibit the behavior of states near the bottom of a band, whereas the state which represented the bottom of the second band at zero field behaves like a state near the top of a band. The absolute cutoff thus seemed to effect an interband transfer that is not present when the cutoff condition is relaxed.

Figures 5(c) and (d) can now be examined together and compared with figures 10(b), (c), and (d) in reference 1. The potential for the state in figure 5(c) of this report is almost exactly the same as for the states in figure 10(b), whereas the magnetic field in 5(d) is about midway between those in figures 10(c) and (d) of reference 1. The suggested comparison shows that the behavior of the states is changed very little by relaxing of the cutoff condition. As asserted in the description of the model, at high magnetic fields, the effect of the cutoff should not be very strong, and this is precisely what the results confirm. In particular, the phenomenon of Blount breakdown and the

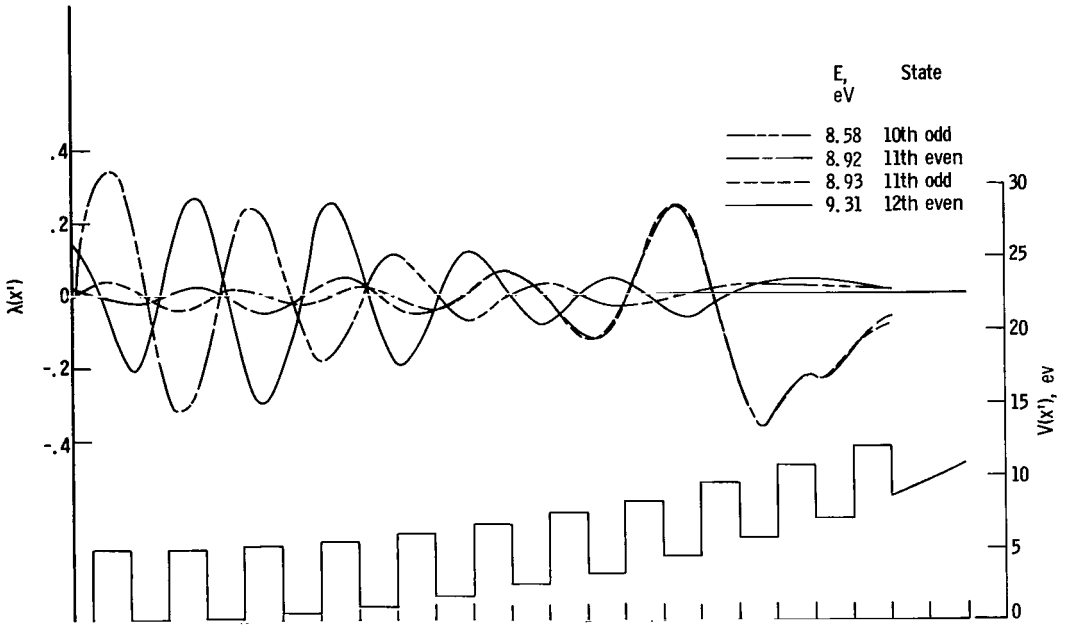

(a) Magnetic field strength, 3.0 kilotesla (well below Blount breakdown).

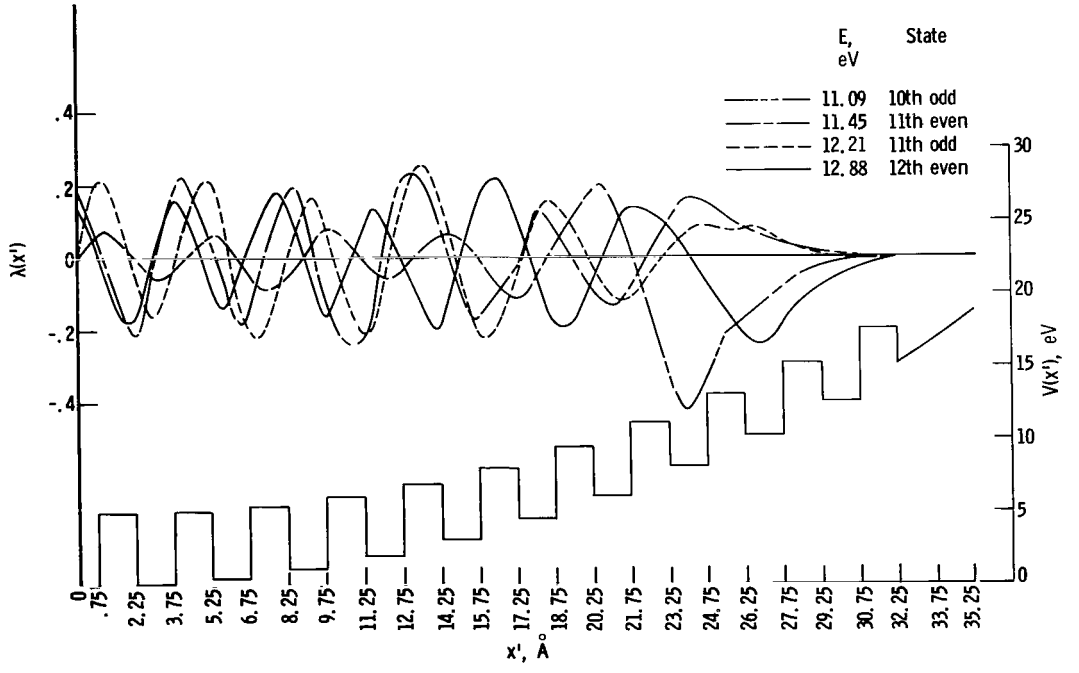

(b) Magnetic field strength, 4.0 kilotesla.

Figure 5. - Wave functions for well depth of 5 electron volts.

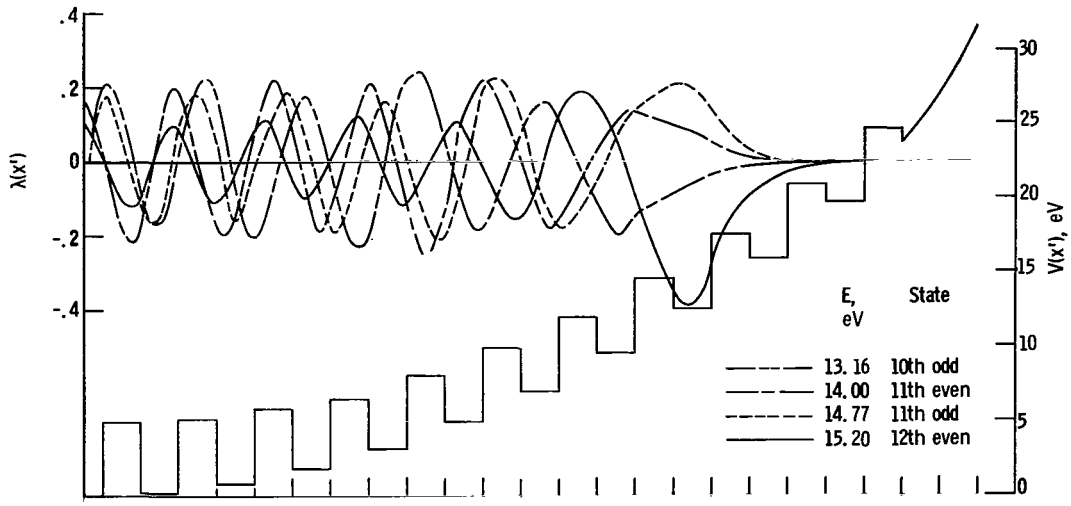

(c) Magnetic field strength, 5.0 kilotesla.

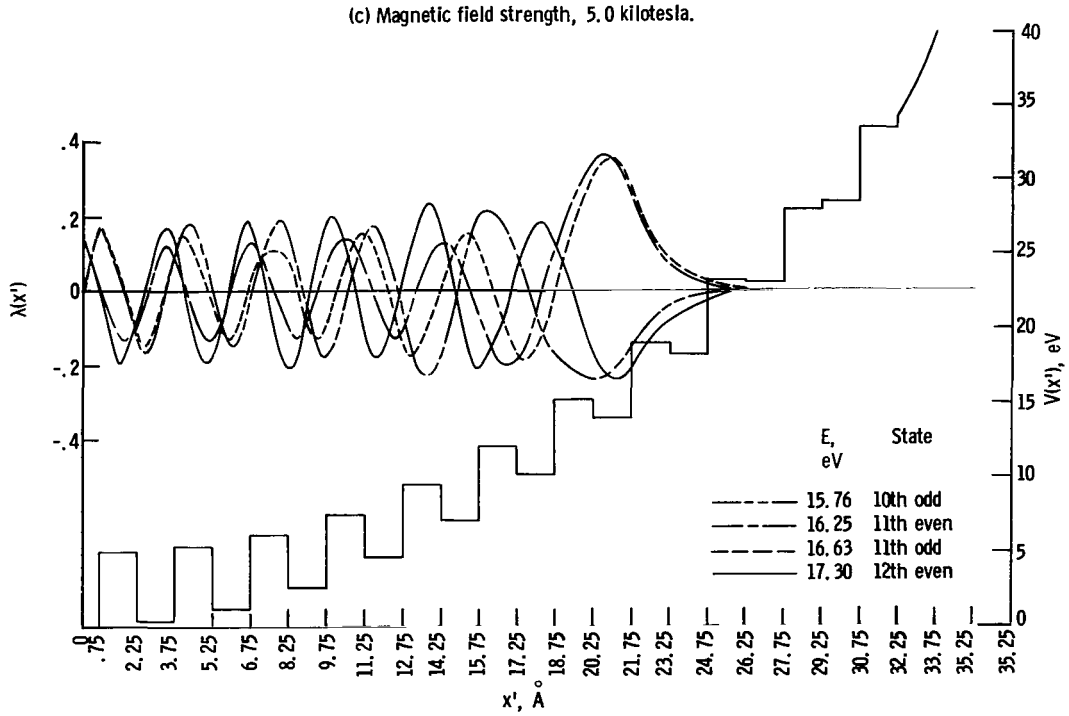

(d) Magnetic field strength, 6.0 kilotesla (near Blount breakdown).

Figure 5. - Concluded.

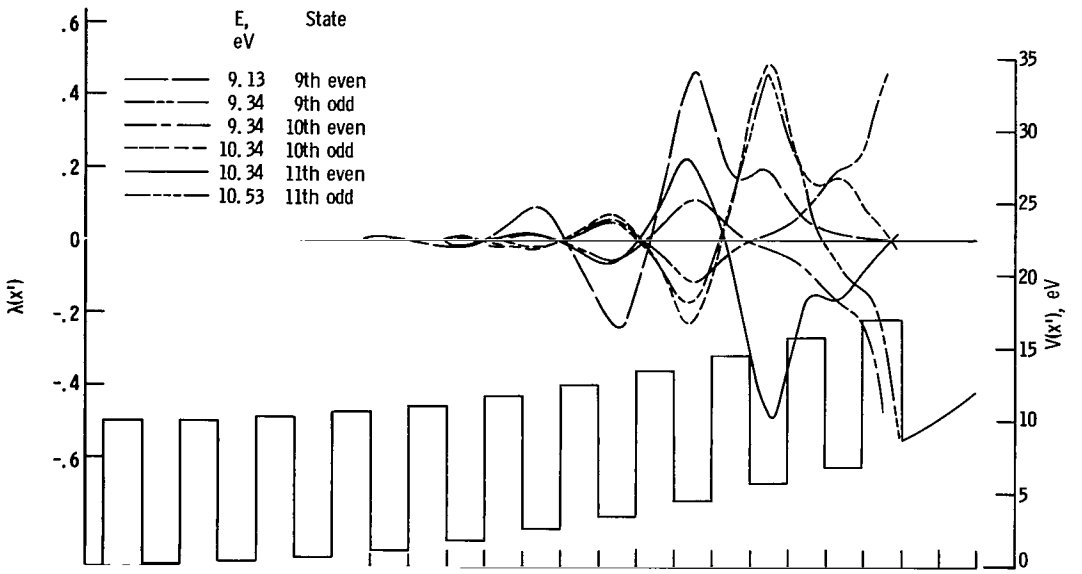

(a) Magnetic field strength, 3 kilotesla (well below Blount breakdown).

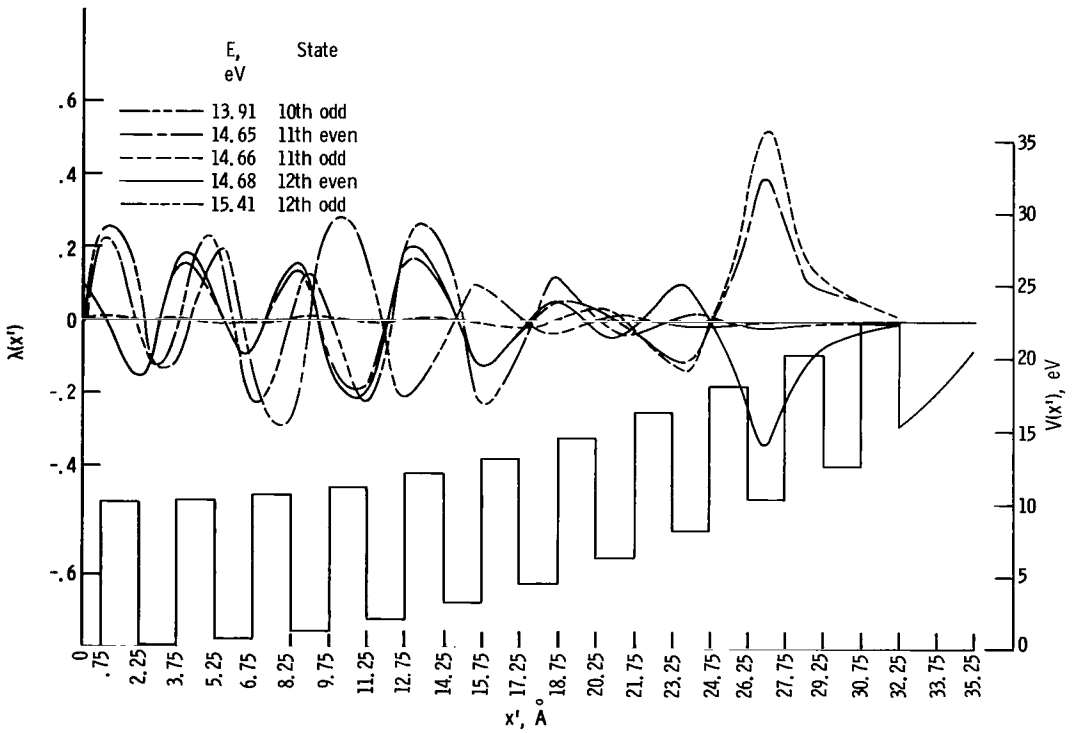

(b) Magnetic field strength, 4 kilotesla.

Figure 6. - Wave functions for well depth of 10 electron volts.

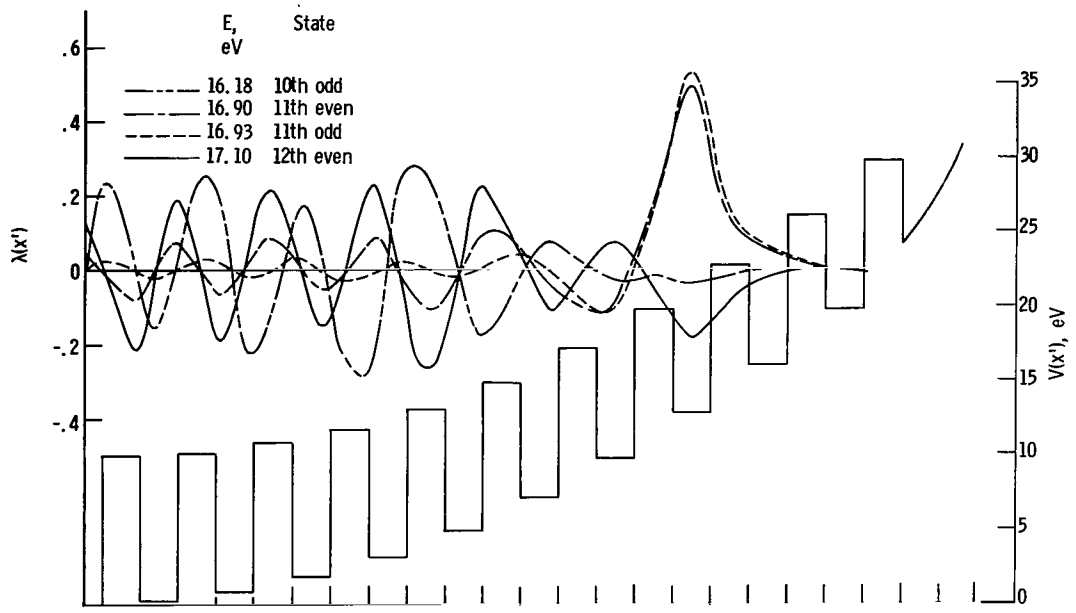

(c) Magnetic field strength, 5 kilotesla.

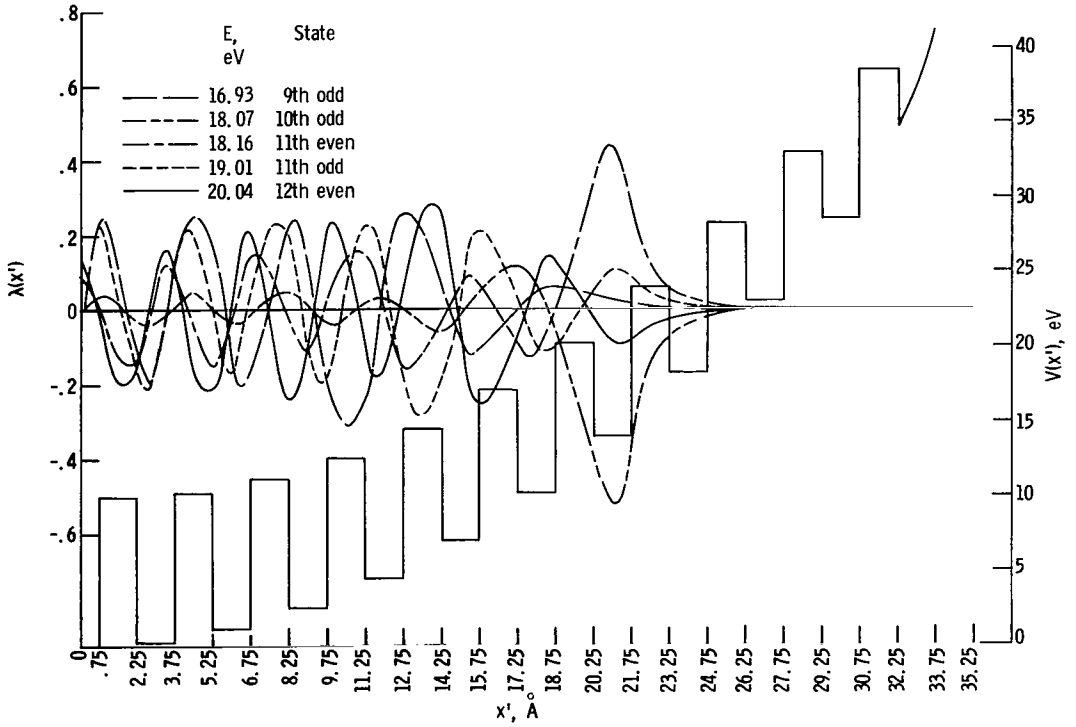

(d) Magnetic field strength, 6 kilotesla.

Figure 6. - Continued.

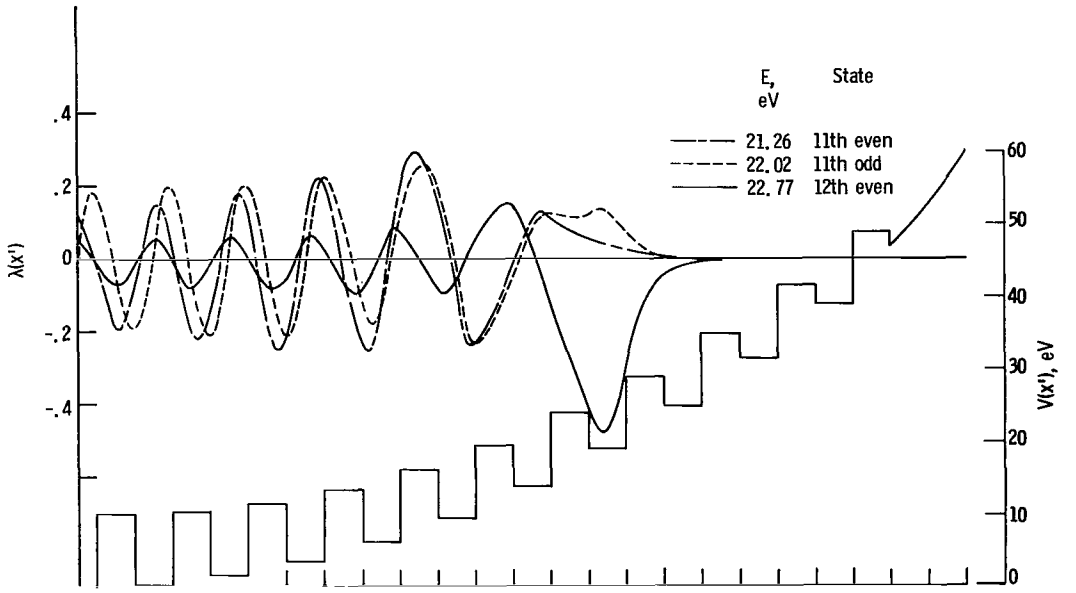

(e) Magnetic field strength, 7 kilotesla.

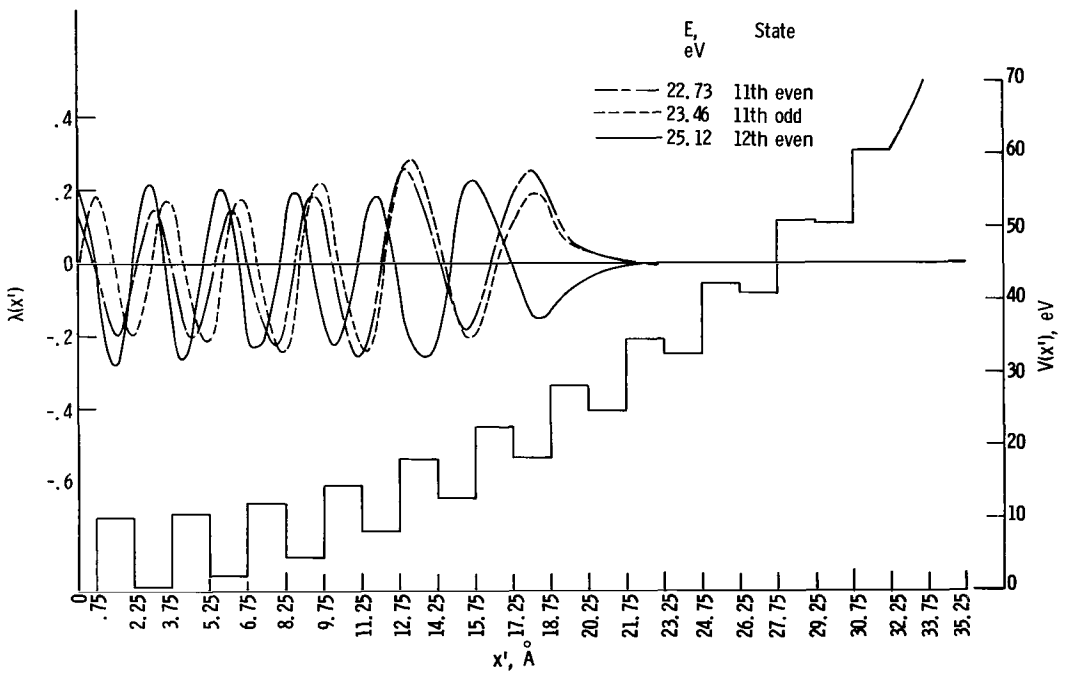

(f) Magnetic field strength, 8 kilotesla.

Figure 6. - Concluded.

disappearance of the effect of the periodic potential is retained upon the relaxation of the cutoff condition.

The discussion of the $V_0 = 10$ case may be prefaced by some pertinent remarks. First, improved computations enabled a more complete set of wave functions to be presented here than was available in reference 1. However, some eigenvalues still did not have sufficiently small D_N values to permit their use in the computation of wave functions. The fact that the set of wave functions for $V_0 = 10$ was relatively incomplete in reference 1 makes it difficult to compare the wave functions with and without the cutoff for this case. What comparison is possible, however, is in agreement with the general ideas presented herein. Secondly, the larger zero field energy gap would tend to require higher magnetic fields to get interband transfer and other wave function behavior similar to the $V_0 = 5$ behavior.

Figure 6(a) (H = 3.0 kilotesla) exhibits the effect of the cutoff very strikingly. A comparison of this figure with figure 5 of reference 1 (which shows wave functions at H = 3.1 kilotesla) shows that the cutoff indeed forced the wave functions to zero near the end of the chain. This effect was so strong that it masked other effects (such as band effects) which might otherwise have been manifest. Also, the eigenvalues themselves were pushed noticeably higher (the states flanking the energy gap were displaced upwards.)

As shown in figure 6(b), when H = 4.0 kilotesla, the wave functions behave in a manner qualitatively similar to those in figure 5(a). The 13.91-electron-volt state is clearly in the second band, the next two are back in the upper part of the first band, and finally the second band states continue to fill up.

Figures 6(c) to 6(f) show the wave functions as H goes from 5.0 to 8.0 kilotesla. The same general behavior is shown by the eigenstates as for the shutdown $V_0 = 5.0$-electron-volt potential wells. Interband transfers show up rather well at the lower magnetic fields; then, as H increases, the evidence of the band structure gradually disappears until at 7.0 kilotesla no remnant of this structure remains. It should be noted that the effects of the periodic part of the potential became small at values of H considerably less than H_B (see fig. 3(b)). This phenomenon might not be quite the same as Blount breakdown; it may rather be a precursor of it.

SUMMARY OF RESULTS

A one-dimensional model has been examined to try to follow some details of the magnetic breakdown process. The model is that of an electron in a uniform magnetic field H_z and a one-dimensional transverse chain of 20 periodic square wells. This model is an improvement over a previous one which cut off the chain by means of an infinite potential at each end.

Exact solutions were obtained for both the eigenvalues and wave functions. Examination of the wave functions showed that, for comparatively small magnetic fields, at a fixed magnetic field and periodic well depth V_0 the behavior of the eigenstates admits a rather consistent interpretation in terms of an inter-

band transfer of characteristics between bands. As the magnetic field is increased, however, the band effects become less pronounced. For V_0 = 5 electron volts, the value of the magnetic field at which such band structures effects become unimportant is the Blount breakdown value H_B. For the deep wells (V_0 = 10 eV), the magnetic field strengths are still quite a bit lower than the H_B values, which indicates that the system may be in some condition which is a sort of precursor of an actual magnetic breakdown state.

Lewis Research Center,
National Aeronautics and Space Administration,
Cleveland, Ohio, October 22, 1965.

APPENDIX A

MATCHING CONDITIONS AND DERIVATION OF EIGENVALUES

The matching conditions up to the N^{th} hill are the same as those in reference 1 and are found in appendix A therein. In the N^{th} hill, however,

$$\lambda_N^h(x') = A_N^h \begin{Bmatrix} \frac{1}{G_N^h} \sinh G_N^h \left[x' - (Na + w)\right] \\ x' - (Na + w) \\ \frac{1}{G_N^h} \sin G_N^h \left[x' - (Na + w)\right] \end{Bmatrix} + B_N^h \begin{Bmatrix} \cosh G_N^h \left[x' - (Na + w)\right] & g_N^h < 0 \\ 1 & g_N^h = 0 \\ \cos G_N^h \left[x' - (Na + w)\right] & g_N^h > 0 \end{Bmatrix} \quad (A1)$$

and

$$\frac{d}{dx'} \lambda_N^h(x') = A_N^h \begin{Bmatrix} \cosh G_N^h \left[x' - (Na + w)\right] \\ 1 \\ \cos G_N^h \left[x' - (Na + w)\right] \end{Bmatrix} + B_N^h G_N^h \begin{Bmatrix} \sinh G_N^h \left[x' - (Na + w)\right] & g_N^h < 0 \\ 0 & g_N^h = 0 \\ -\sin G_N^h \left[x' - (Na + w)\right] & g_N^h > 0 \end{Bmatrix} \quad (A2)$$

In the pure magnetic region, $x' > (N + 1)a - w$,

$$\lambda_M(x') = A_M D_\nu(\xi) \quad (A3)$$

and from reference 2,

$$\frac{d}{dx'} \lambda_M(x') = A_M \sqrt{\frac{2m\omega_c}{\hbar}} \left[\frac{\xi}{2} D_\nu(\xi) - D_{\nu+1}(\xi)\right] \quad (A4)$$

The matching conditions then become

$$A_N^h C_R A_N^h + B_N^h C_R B_N^h = A_M C_L A_M \tag{A5}$$

$$A_N^h C_R' A_N^h + B_N^h C_R' B_N^h = A_M C_L' A_M \tag{A6}$$

where

$$C_L A_M = D_\nu \left\{ \sqrt{\frac{2m\omega_c}{\hbar}} \left[(N + 1)a - w \right] \right\} = D_\nu(\xi_M) \tag{A7}$$

$$C_L' A_M = \sqrt{\frac{2m\omega_c}{\hbar}} \left[\frac{\xi_M}{2} D_\nu(\xi_M) - D_{\nu+1}(\xi_M) \right] \tag{A8}$$

$$\xi_M = \sqrt{\frac{2m\omega_c}{\hbar}} \left[(N + 1)a - w \right] \tag{A9}$$

and the other quantities appear in appendix A of reference 1.

With these changes, the determinantal compatibility condition is obtained by setting equal to zero the following determinant D_N, which corresponds to equation (A31) in reference 1 (note that this is specifically for the case of even functions):

$$\begin{array}{cccccccc|ccc}
A_M & A_N^h & B_N^h & A_N^w & B_N^w & A_{N-1}^h & B_{N-1}^h & \cdots & A_0^h & B_0^h & B_0^w \\
\hline
-C_L A_M & C_R A_N^h & C_R B_N^h & 0 & 0 & 0 & 0 & \cdots & 0 & 0 & 0 \\
-C_L' A_M & C_R' A_N^h & C_R' B_N^h & 0 & 0 & 0 & 0 & \cdots & 0 & 0 & 0 \\
0 & 0 & -1 & C_R A_N^w & C_R B_N^w & 0 & 0 & \cdots & 0 & 0 & 0 \\
0 & -1 & 0 & C_R' A_N^w & C_R' B_N^w & 0 & 0 & \cdots & 0 & 0 & 0 \\
0 & 0 & 0 & 0 & -1 & C_R A_{N-1}^h & C_R B_{N-1}^h & \cdots & 0 & 0 & 0 \\
0 & 0 & 0 & -1 & 0 & C_R' A_{N-1}^h & C_R' B_{N-1}^h & \cdots & 0 & 0 & 0 \\
0 & 0 & 0 & 0 & 0 & 0 & -1 & \cdots & 0 & 0 & 0 \\
0 & 0 & 0 & 0 & 0 & -1 & 0 & \cdots & 0 & 0 & 0 \\
\vdots & \vdots & \vdots & \vdots & \vdots & \vdots & \vdots & \cdots & \vdots & \vdots & \vdots \\
0 & 0 & 0 & 0 & 0 & 0 & 0 & \cdots & C_R A_0^h & C_R B_0^h & 0 \\
0 & 0 & 0 & 0 & 0 & 0 & 0 & \cdots & C_R' A_0^h & C_R' B_0^h & 0 \\
0 & 0 & 0 & 0 & 0 & 0 & 0 & \cdots & 0 & -1 & \cos wG_0^w \\
0 & 0 & 0 & 0 & 0 & 0 & 0 & \cdots & -1 & 0 & -G_0^w \sin wG_0^w
\end{array} \tag{A10}$$

The procedure for evaluating D_N is the same as was used in reference 1 but will be sketched here for completeness. First the quantities S_0^w and $\bar{S}_0^w$ are defined as follows:

For even solutions:

$$\left.\begin{aligned} S_0^w &= \cos wG_0^w \\ \bar{S}_0^w &= -G_0^w \sin wG_0^w \end{aligned}\right\} \tag{A11}$$

For odd solutions:

$$\left.\begin{aligned} S_0^w &= \frac{1}{G_0^w} \sin wG_0^w \\ \bar{S}_0^w &= \cos wG_0^w \end{aligned}\right\} \tag{A12}$$

Then equations (A13) are used alternately with equations (A14) up to and including $n = N$:

$$\left.\begin{aligned} S_n^h &= C_R A_n^h \bar{S}_n^w + C_R B_n^h S_n^w \\ \bar{S}_n^h &= C_R' A_n^h \bar{S}_n^w + C_R' B_n^h S_n^w \end{aligned}\right\} \tag{A13}$$

$$\left.\begin{aligned} S_n^w &= C_R A_n^w \bar{S}_{n-1}^h + C_R B_n^w S_{n-1}^h \\ \bar{S}_n^w &= C_R' A_n^w \bar{S}_{n-1}^h + C_R' B_n^w S_{n-1}^h \end{aligned}\right\} \tag{A14}$$

where

$$C_R^{\pm} \bar{A}_n^w = \begin{cases} \dfrac{1}{G_n^w} \sinh 2wG_n^w \\ 2w \\ \dfrac{1}{G_n^w} \sin 2wG_n^w \end{cases} \tag{A15}$$

$$C_R^{\overline{O}+}B_n^w = C_R'^{\overline{O}+}A_n^w = \begin{cases} \cosh 2wG_n^w \\ 1 \\ \cos 2wG_n^w \end{cases} \tag{A16}$$

$$C_R'^{\overline{O}+}B_N^w = \begin{cases} G_n^w \sinh 2wG_n^w \\ 0 \\ -G_n^w \sin 2wG_n^w \end{cases} \tag{A17}$$

$$C_R^{\overline{O}+}A_n^h = \begin{cases} \frac{1}{G_n^h} \sinh 2hG_n^h \\ 2h \\ \frac{1}{G_n^h} \sin 2hG_n^h \end{cases} \tag{A18}$$

$$C_R^{\overline{O}+}B_n^h = C_R'^{\overline{O}+}A_n^h = \begin{cases} \cosh 2hG_n^h \\ 1 \\ \cos 2hG_n^h \end{cases} \tag{A19}$$

$$C_R'^{\overline{O}+}B_n^h = \begin{cases} G_n^h \sinh 2hG_n^h \\ 0 \\ -G_n^h \sin 2hG_n^h \end{cases} \tag{A20}$$

Finally,

$$D_N = -\bar{S}_N^h C_L A_M + S_N^h C_L' A_M = 0 \tag{A21}$$

These quantities are used in the computation of D_N. When D_N is deemed to be sufficiently close to zero, the value of E which was used in that computation is considered to be an eigenvalue for the given combination of V_O and H_Z.

APPENDIX B

COMPUTATION OF WEBER FUNCTIONS

Parabolic cylinder functions (or Weber functions) oscillate with amplitudes proportional to $\sqrt{\Gamma(\nu+\frac{1}{2})}$. From equation (14) it can be seen that ν can be very large in these computations and, in fact, became large enough so that the numbers in the computations would sometimes fall outside the range of the Lewis 7094. For this reason, a "reduced" Weber function with an amplitude not exceeding one unit was used in this computation (ref. 6). A description of the use of these functions follows.

The superscript R denotes reduced. Then the determinantal compatibility condition $D_N = 0$ can be written as

$$D_N = \sqrt{\Gamma(\nu + \tfrac{1}{2})}\ D_N^R = 0 \tag{B1}$$

It may be noted that for the values of E in this report, $\Gamma(\nu + \frac{1}{2})$, will always be greater than zero so that D_N and D_N^R vanish at the same values of E. Here

$$D_N^R = -\bar{S}_N^h C_L A_M^R + S_N^h C_L' A_M^R \tag{B2}$$

where

$$C_L A_M^R = \frac{1}{\sqrt{\Gamma(\nu+\frac{1}{2})}}\ C_L A_M = \frac{1}{\sqrt{\Gamma(\nu+\frac{1}{2})}}\ D_\nu(\xi_M) \tag{B3}$$

$$C_L' A_M^R = \frac{C_L' A_M^R}{\sqrt{\Gamma(\nu+\frac{1}{2})}} = \sqrt{\frac{2m\omega_c}{\hbar}}\left[\frac{\xi_M}{2} D_\nu^R(\xi_M) - \sqrt{\frac{\Gamma(\nu+\frac{3}{2})}{\Gamma(\nu+\frac{1}{2})}}\ D_{\nu+1}(\xi_M)\right]$$

$$= \sqrt{\frac{2m\omega_c}{\hbar}}\left[\frac{\xi_M}{2} D_\nu^R(\xi_M) - \sqrt{\nu+\tfrac{1}{2}}\ D_{\nu+1}^R(\xi_M)\right] \tag{B4}$$

Practical procedures for computing values of high-order Weber functions do not seem to be readily available especially at large arguments (ref. 7), so a procedure for obtaining such values on the Lewis 7094 was developed.

REFERENCES

1. Allen, Gabriel: Magnetic Breakdown in a Finite One-Dimensional Model. NASA TN D-2554, 1964.

2. Erdelyi, Arthur; Magnus, Wilhelm; Oberhettinger, Fritz; and Tricomi, Francesco G., eds.: Higher Transcendental Functions. McGraw-Hill Book Co., Inc., 1953, ch. VIII.

3. Messiah, Albert: Quantum Mechanics. Vol. I. North Holland Pub. Co., 1961, p. 113.

4. Peierls, Rudolfh Ernst: Quantum Theory of Solids. Clarendon Press (Oxford), 1955, pp. 150-152.

5. Allen, G.: Band Structures of One-Dimensional Crystals with Square-Well Potentials. Phys. Rev., vol. 91, no. 3, Aug. 1, 1953, pp. 531-533.

6. Jahnke, Eugene; Emde, Fritz; and Lösch, Friederich: Tables of Higher Functions. Sixth ed., McGraw-Hill Book Co., Inc., 1960, p. 103.

7. Abramowitz, Milton; and Stegun, Irene A.: Handbook of Mathematical Functions. Appl. Math. Ser. No. 55, Nat. Bur. Stds., 1964, ch. 19.

NASA-Langley, 1966 E-3188

"The aeronautical and space activities of the United States shall be conducted so as to contribute . . . to the expansion of human knowledge of phenomena in the atmosphere and space. The Administration shall provide for the widest practicable and appropriate dissemination of information concerning its activities and the results thereof."

—NATIONAL AERONAUTICS AND SPACE ACT OF 1958

NASA SCIENTIFIC AND TECHNICAL PUBLICATIONS

TECHNICAL REPORTS: Scientific and technical information considered important, complete, and a lasting contribution to existing knowledge.

TECHNICAL NOTES: Information less broad in scope but nevertheless of importance as a contribution to existing knowledge.

TECHNICAL MEMORANDUMS: Information receiving limited distribution because of preliminary data, security classification, or other reasons.

CONTRACTOR REPORTS: Technical information generated in connection with a NASA contract or grant and released under NASA auspices.

TECHNICAL TRANSLATIONS: Information published in a foreign language considered to merit NASA distribution in English.

TECHNICAL REPRINTS: Information derived from NASA activities and initially published in the form of journal articles.

SPECIAL PUBLICATIONS: Information derived from or of value to NASA activities but not necessarily reporting the results of individual NASA-programmed scientific efforts. Publications include conference proceedings, monographs, data compilations, handbooks, sourcebooks, and special bibliographies.

Details on the availability of these publications may be obtained from:

SCIENTIFIC AND TECHNICAL INFORMATION DIVISION

NATIONAL AERONAUTICS AND SPACE ADMINISTRATION

Washington, D.C. 20546